



On the Limitations of Breakthrough Curve Analysis in Fixed-Bed Adsorption

James C. Knox



Introduction

- Fixed Beds used for Separation via Gas Adsorption in Numerous Applications, for example:
 - Chemical processing industry (petrochemicals, foods, medicines, etc.)
 - Thermochemical energy storage
 - DOE funded efforts to develop affordable flue gas CO₂ capture systems
 - Atmospheric control in habitable volumes
- Generally multiple bed cyclic processes such as pressure swing adsorption (PSA) or temperature swing adsorption (TSA)
- Direct simulation of the highly random sorbent particle packing and small-scale features of the flow between particles in a fixed-bed is CPU intensive
- To achieve cyclic steady-state in a process simulation, as required for process design, 1-D models are utilized

Fluid flow in a packed bed – studies in catalyst reactor design

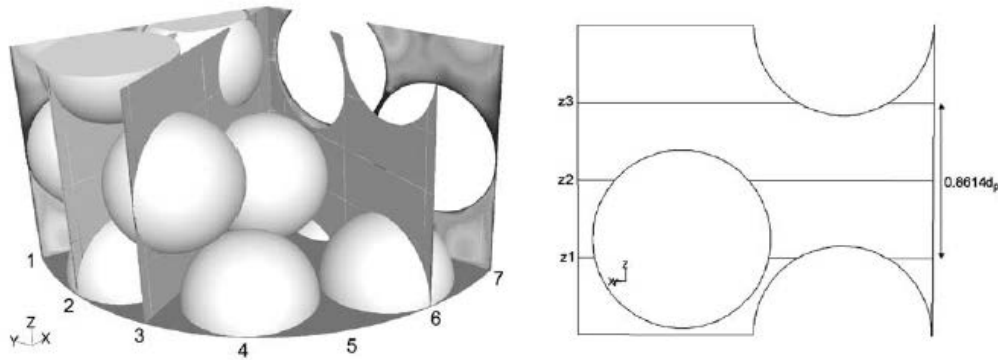


FIG. 10. Comparison section with seven tangential planes and axial profile lines indicated.

PACKED TUBULAR REACTOR MODELING AND CATALYST DESIGN 347

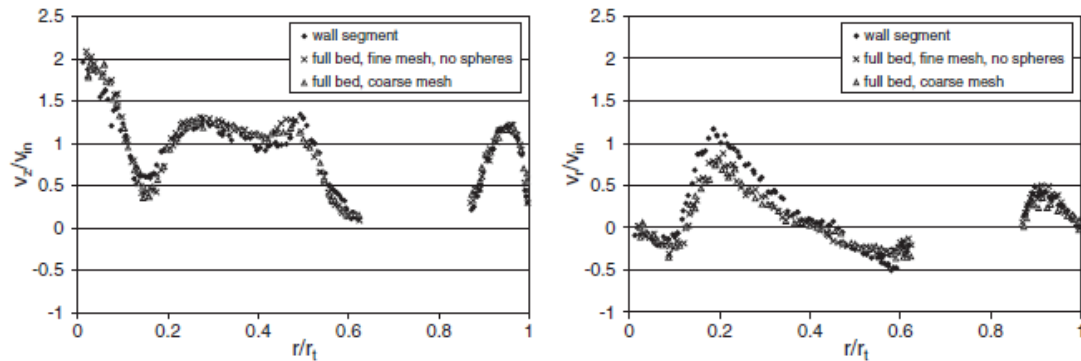


FIG. 11. Full-bed and WS mesh comparisons of axial and radial velocity components (at Z3).

Dixon AG, Nijemeisland M, Stitt EH. Packed Tubular Reactor Modeling and Catalyst Design using Computational Fluid Dynamics. In: Guy BM, ed. Advances in Chemical Engineering. Vol Volume 31: Academic Press; 2006:307-389.

10/6/16

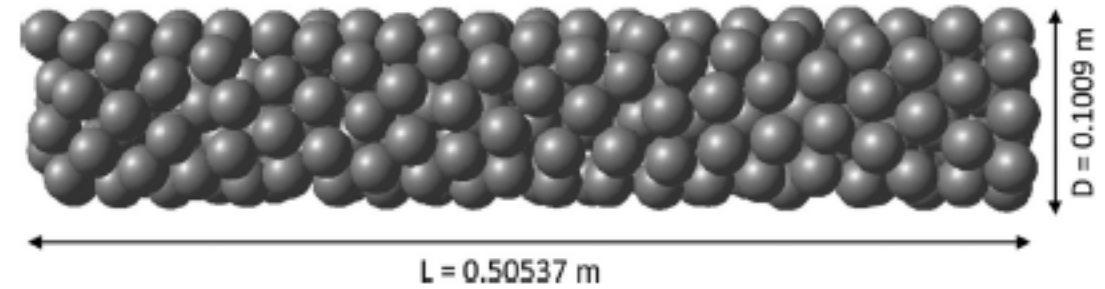


Figure 9. Close-up analysis of boxed regions from Figure 8 with $N = 3.96$ and $Re = 240$: (a) velocity vectors colored by axial velocity (m/s), (b) velocity vectors colored by radial velocity (m/s), and (c) temperature contours (K).

Behnam M, Dixon AG, Nijemeisland M, Stitt EH. A New Approach to Fixed Bed Radial Heat Transfer Modeling Using Velocity Fields from Computational Fluid Dynamics Simulations. *Ind Eng Chem Res.* 2013/11/06 2013;52(44):15244-1526



Principle Equations in 1-D Model

$$\frac{\partial c}{\partial t} + \left(\frac{1-\varepsilon}{\varepsilon} \right) \frac{\partial \bar{q}}{\partial t} - D_L \frac{\partial^2 c}{\partial x^2} = - \frac{\partial v_i c}{\partial x}$$

$$\frac{\partial \bar{q}}{\partial t} = k_g (q^* - \bar{q})$$

$$\varepsilon a_f \rho_f c_{pf} \frac{\partial T_f}{\partial t} - \varepsilon a_f k_{eff} \frac{\partial^2 T_f}{\partial x^2} = -\varepsilon a_f \rho_f v_i c_{pf} \frac{\partial T_f}{\partial x} + a_f a_s h_s (T_s - T_f) + P_i h_i (T_w - T_f)$$

$$(1-\varepsilon) \rho_s c_{ps} \frac{\partial T_s}{\partial t} = a_f a_s h_s (T_f - T_s) - (1-\varepsilon) a_f \lambda \frac{\partial q}{\partial t}$$

$$a_w \rho_w c_{pw} \frac{\partial T_w}{\partial t} - a_w k_w \frac{\partial^2 T_w}{\partial x^2} = P_i h_i (T_f - T_w) + P_a h_a (T_a - T_w)$$

$$n = \frac{ap}{[1+(bp)^t]^{1/t}}; \quad b = b_0 \exp(E/T); \quad a = a_0 \exp(E/T); \quad t = t_0 + c/T$$

$$\frac{1}{Pe} = \frac{20}{\varepsilon} \left(\frac{D}{2vR_p} \right) + \frac{1}{2} = \frac{20}{ReSc} + \frac{1}{2}$$

$$\frac{1}{Pe} = \frac{0.73\varepsilon}{ReSc} + \frac{1}{2 \left(1 + \frac{13 \cdot 0.73\varepsilon}{ReSc} \right)} \quad 0.0377 < 2R_p < 0.607 \text{ cm}$$

$$h_i = \frac{k_f}{2R_i} Nu \quad \text{with} \quad Nu = 2.03 Re^{0.8} \exp \left(-6 \frac{R_p}{R_i} \right)$$

$$c_p = a_o + a_1 T_f + a_2 T_f^2 + a_3 T_f^3$$

$$Sh = 2 + 1.1 Sc^{1/3} Re^{0.6} \quad h_s = \frac{ShD}{2R_p}$$

$$k_e = k_f \left(\frac{k_s}{k_f} \right)^n \quad \text{with} \quad n = 0.280 - 0.757 \log_{10} \varepsilon - 0.057 \log_{10} \left(\frac{k_s}{k_f} \right)$$

$$k_{eff} = k_f \left(\frac{k_e}{k_f} + 0.75 Pr Re \right) \quad \text{where} \quad Pr = \frac{c_p \mu}{\rho_f k_f}$$

All variables in Mass and Heat Balance Equations are determined except D_L , k_n , and h_o



Virtual Adsorption Test Suite

- Matlab/COMSOL Component:
 - Inputs engineering data from actual or proposed test (breakthrough or cyclic)
 - Based on inlet conditions, calculates gas properties required for heat and mass transfer correlations
 - Builds requested PDE-based model with specified grid spacing, time steps, cycles etc.
 - Hands off model to COMSOL Multiphysics (used as PDE Solver) for execution and retrieves results when complete
 - Has been used with NASA X-TOOLSS (genetic algorithms) for parameter optimization
 - Allows for multi-variable parametric runs, and compares SSR of results vs. test data for parameter optimization
 - Generates paper-ready plots including plot over of test data
- Mathcad Component:
 - Provides independent verification of all calculations in Matlab component
 - Provides sensitivity analysis of correlations to temperature and concentration changes expected during a simulation

Centerline LDF fits database.

FileRecordCalculationsCOMSOL

General Information

Record Number5

Description

Centerline Fitting

Data Source

MSMBT Test on 04-07-94M

Sorbent Type

Grace Davison 5A Grade 5

Test Stand

MSMBT Cylindrical Column

Run Identifier

W-F LDF after fit to center

Notes

Observations

Standard Temp[degC]

0

Standard Press[kPa]

101.325

Adsorption Conditions

Ads Flow Rate[slpm]

28.26

Ads Initial Temp[degC]

23.35

Ads Inlet Temp[degC]

22.35

Constant or Timelined

Constant

CO2/H2O/O2/N2[kPa]

0 0.805 0 107.24

Constant or Timelined

Constant

Ads Inlet Air[kPa]

0

Ads Inlet He[kPa]

0

Ads Sorbate

H2O

Ads Initial Conc[mol/m^3]

0.001

Ads Initial Load[mol/m^3]

1

Sorbate MolWt[kg/mol]

Desorption Conditions

Des Flow Rate[l/min]

28.04

Des Initial Temp[degC]

22.406

Constant or Timelined

Constant

Des Inlet Temp[degC]

22.406

CO2/H2O/O2/N2[kPa]

0 0.805 0 106.064

Constant or Timelined

Constant

Des Inlet Air[kPa]

0

Des Inlet He[kPa]

0

Des Sorbate

H2O

Des Initial Conc[mol/m^3]

0.001

Des Initial Load[mol/m^3]

1

Canister Information

Free Flow Area[cm^2]

17.814

Canister CS Area[cm^2]

2.45

Can Inner Perimeter[cm]

14.96

Can Outer Perimeter[cm]

15.96

Bed Length[m]

0.254

Void Fraction

0.33

Wall Void Fraction

1

Can Cond[W/(m^*K)]

16.8

Can Q Capac[J/(kg^*K)]

475

Can Density[kg/m^3]

7833

Ambient Temp[degC]

22.406

Can-Amb H[W/(m^2*K)]

1.685

Sorbent Information

Sorbent Type

5A

Sorbent Mass[g]

0

Part Density[kg/m^3]

1180

Pellet Diameter[mm]

2.32

Pellet Length[mm]

0

Mass Trans Coeff[1/s]

0.00098

Sorb Q Cond[W/(m^*K)]

0.12

Sorb Q Capac[J/(kg^*K)]

1046.7

Heat of Ads[kJ/mol]

-65.1

Inlet Temperature / Error Checking

Constant or Timelined

Timelined

Timeline File Name

Templn.txt

Conc Test Data File

Conc 975 1000 SSE.txt

Gas Temp Test Data File

GasTemp 500 975 SSE.tx

Col Temp Test Data File

none

Scope of Err Check[%]

75 101

Scaling for Err[fraction]

1 1 0.5 0.5 0.5 0.5 0.2 0.2

Simulation Control

Model Name/Solver

PDE FC

Half-Cycle Length[s]

36000

Number of Half Cycles

1

Time Step[s]

30

Node Sep Max[m]

0.001

Node Sep Init[m]

0.0001

Parametric Iterations

1

Parameter Name

AdsAxialDisp

Minimum Value

0.00238473

Maximum Value

0.001

Plot Specifications

Spatial Locations

200

Num of Plot Points

3 3 25 25 25 25

Plot Type

PlotOver

Plots per Page

2

Simulation Data

cWT TgWT ct

Conc Data File

Test Concs for Plots with I

Conc Legends

Inlet Mid Exit Mixed

Gas Temp Data

Test Temps for Plots with

Gas Temp Legends

Inlet Mid Exit

Col Temp Data

none

Col Temp Legends

none

y-axis high limit

1 2 1 1 1 2 1

y-axis low limit

1 2 1 1 1 2 1

Start/End Slope Max

25 100

Legend Location

none none none

ParaBox Location

none none none

Test Data OffSet[s]

0 0 0

Write Sim Data?

no

Adsorption Calculations

Ads Concentrat[mol/m^3]

0.327645

Ads Interstitial Vel[m/s]

0.812856

Ads Bed Loading[mol/kg]

13.0163

Ads Residence Time[s]

0.312478

Ads Stoichio BT Time[m]

495.674

Adsorption Gas Properties

Ads Viscosity[uPa*s]

17.5667

Ads Mol Diff[m^2/s]

2.379e-05

Ads Reynolds Number

43.5252

Ads Schmidt Number

0.601007

Gas Q Cap[kJ/(kg^*K)]

1.048

Axial Cond[W/(m^*K)]

0.671489

Sorbate Q Cap[kJ/(kg^*K)]

1.89756

Sorb-Gas H[W/(m^2*K)]

144.334

Gas-Can H[W/(m^2*K)]

19.9474

Adsorption Mass Transfer

Ads Axial Disp[m^2/s]

0.0023847

Ads Axial Dis Mn[m^2/s]

0.000844941

Ads Axial Dis Mx[m^2/s]

0.00238473

Ads Film Diff[m/s]

0.112096

Ads Film Diff Min[m/s]

0.104927

Ads Film Diff Max[m/s]

0.114299

Adsorption Miscellaneous

Ads Total Press[kPa]

108.045

Ads Mix Mol Wt[g/mole]

27.9385

Ads Gas Dens[kg/m^3]

1.22861

Ads Superfic Vel[m/s]

0.268243

Ads Solid Conc[mol/m^3]

15359.3

Calculations

Equil Work Cap[mol/kg]

0.0042

Equiv Pellet Dia[mm]

2.32

Area to Vol ratio[1/m]

192.529

Void from Sorb Mass

0

Packed Dens[kg/m^3]

790.6

Sorb Mass via Void[g]

357.727

Sim - Test Error

35.5539

Calculated Offset[s]

-1220.3371 -4957.7211

Desorption Calculations

Des Concentrat[mol/m^3]

0.327583

Des Interstitial Vel[m/s]

0.815558

Des Bed Loading[mol/kg]

13.0121

Des Residence Time[s]

0.311443

Des Stoichio BT Time[m]

493.966

Desorption Gas Properties

Des Viscosity[uPa*s]

17.5679

Des Mol Diff[m^2/s]

2.40598e-05

Des Reynolds Number

43.1821

Des Schmidt Number

0.60098

Gas Q Cap[kJ/(mol^*K)]

1.04806

Axial Cond[W/(m^*K)]

0.666838

Sorbate Q Cap[J/(kg^*K)]

1.8976

Sorb-Gas H[W/(m^2*K)]

143.799

Gas-Can H[W/(m^2*K)]

19.8251

Desorption Mass Transfer

Des Axial Disp[m^2/s]

0.00086174

Des Axial Dis Mn[m^2/s]

0.000847087

Des Axial Dis Mx[m^2/s]

0.00240422

Des Film Diff[1/s]

0.112927

Des Film Diff Min[1/s]

0.105579

Des Film Diff Max[1/s]

0.115595

Desorption Miscellaneous

Des Total Press[kPa]

106.869

Des Mix Mol Wt[g/mole]

27.9377

Des Gas Dens[kg/m^3]

1.21498

Des Superfic Vel[m/s]

0.269134

Des Solid Conc[mol/m^3]

15354.3

Toth Isotherm Parameters

Toth a0[mol/kg/kPa]

1.106e-08

Toth b0[1/kPa]

4.714e-10

Toth E[K]

9955

Toth to

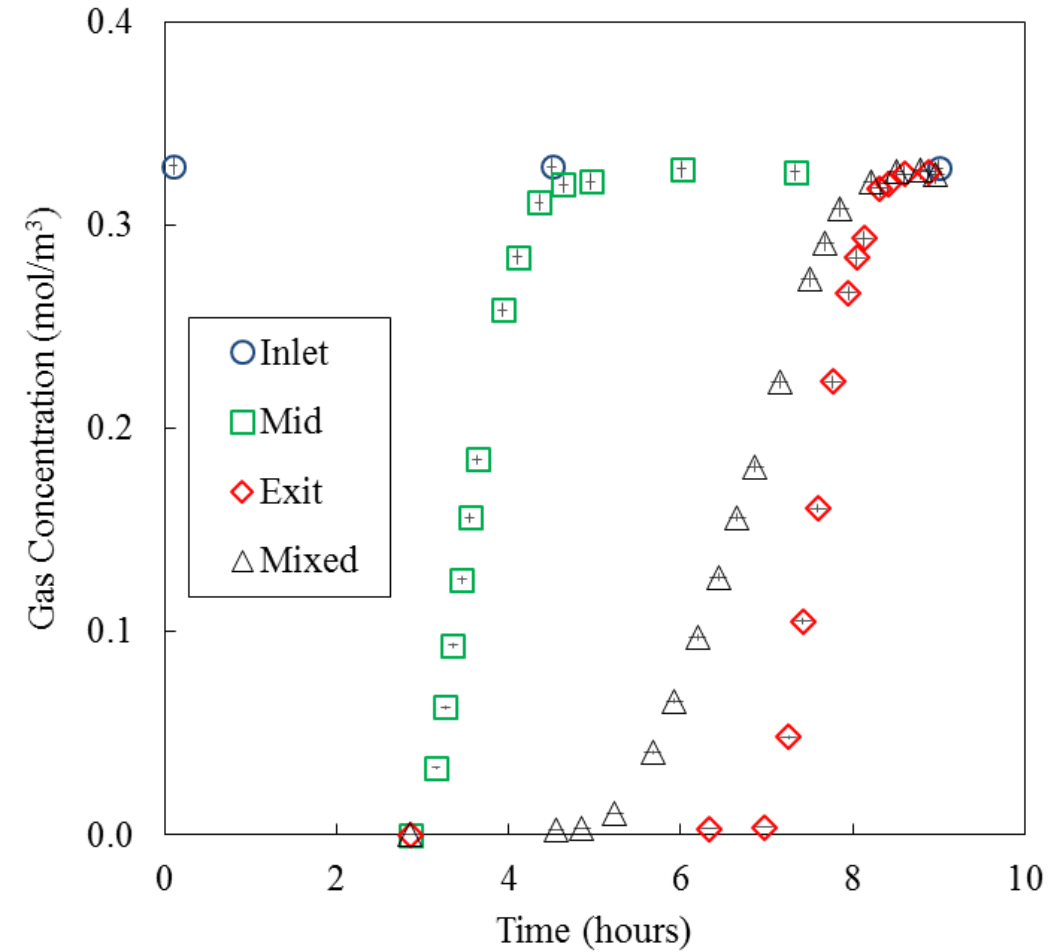
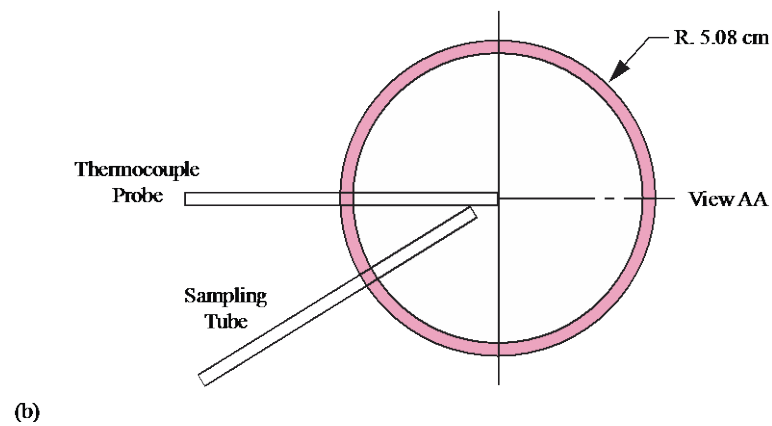
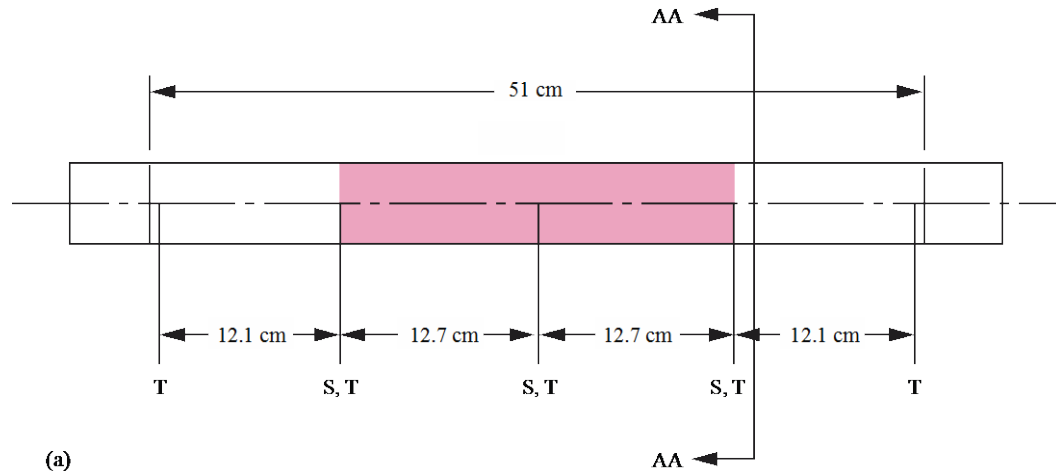
0.3548

Toth c[K]

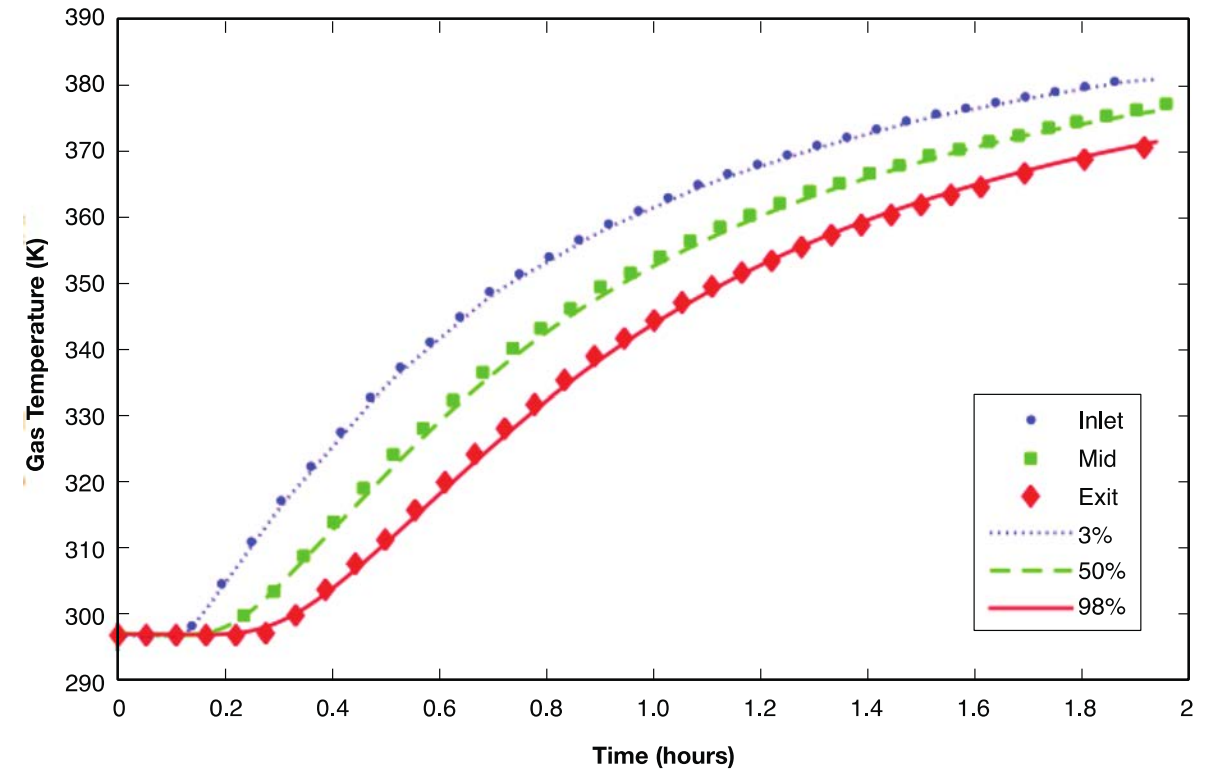
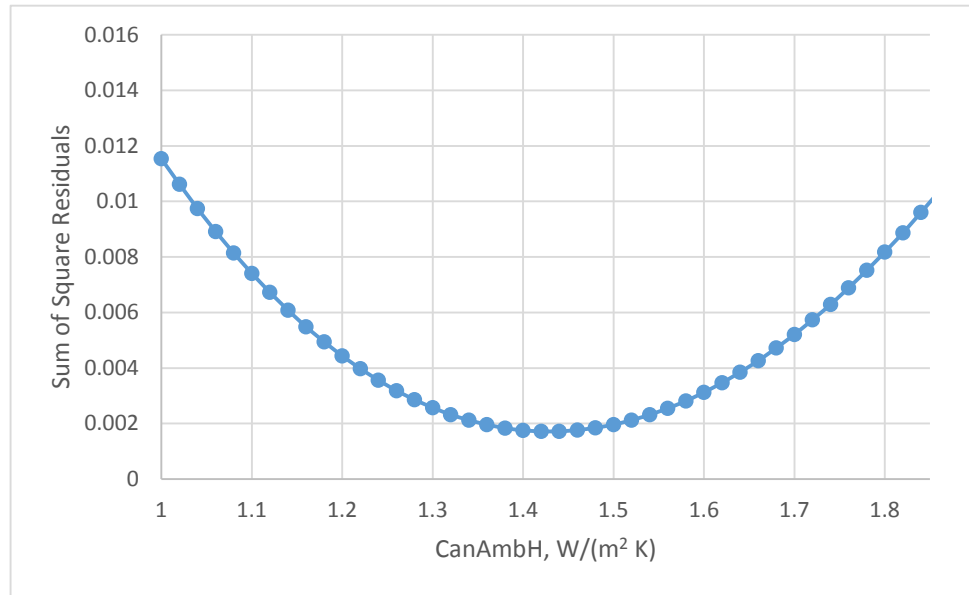
-51.14



Experimental Results for H₂O on 5A

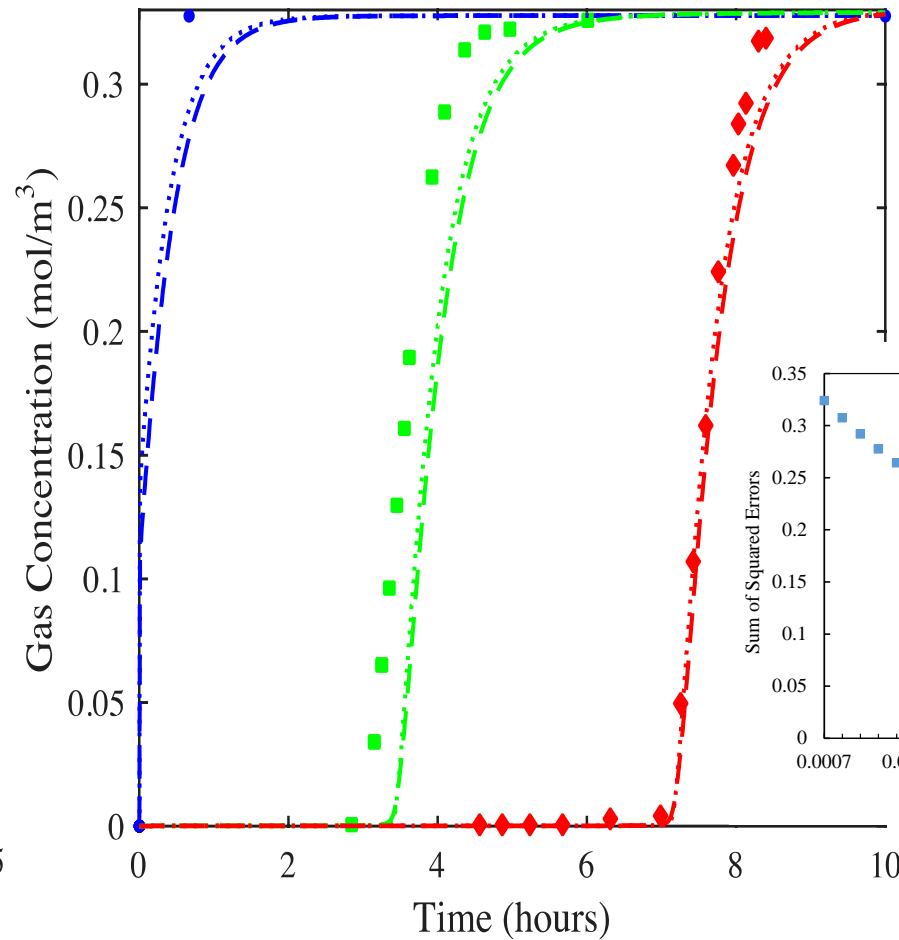
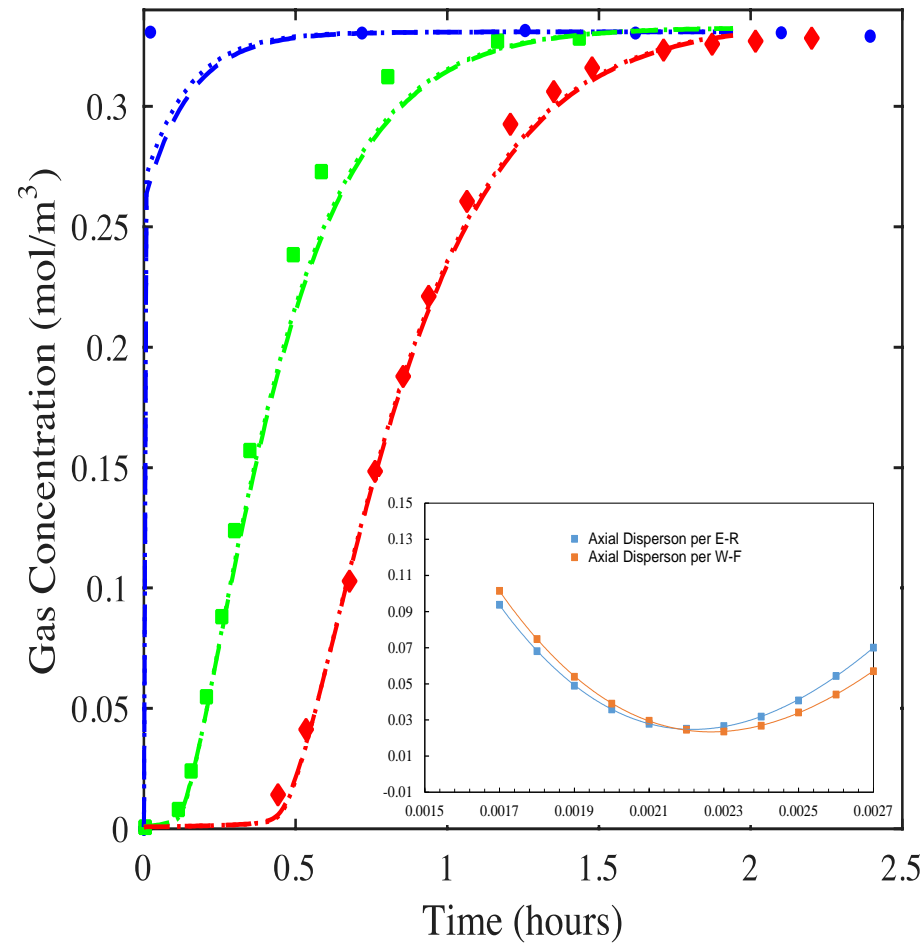


Step 1: Wall to Ambient Heat Transfer Coefficient



h_o is empirically derived via a Thermal Characterization Test

Step 2: Linear Driving Force Mass Transfer Coefficient

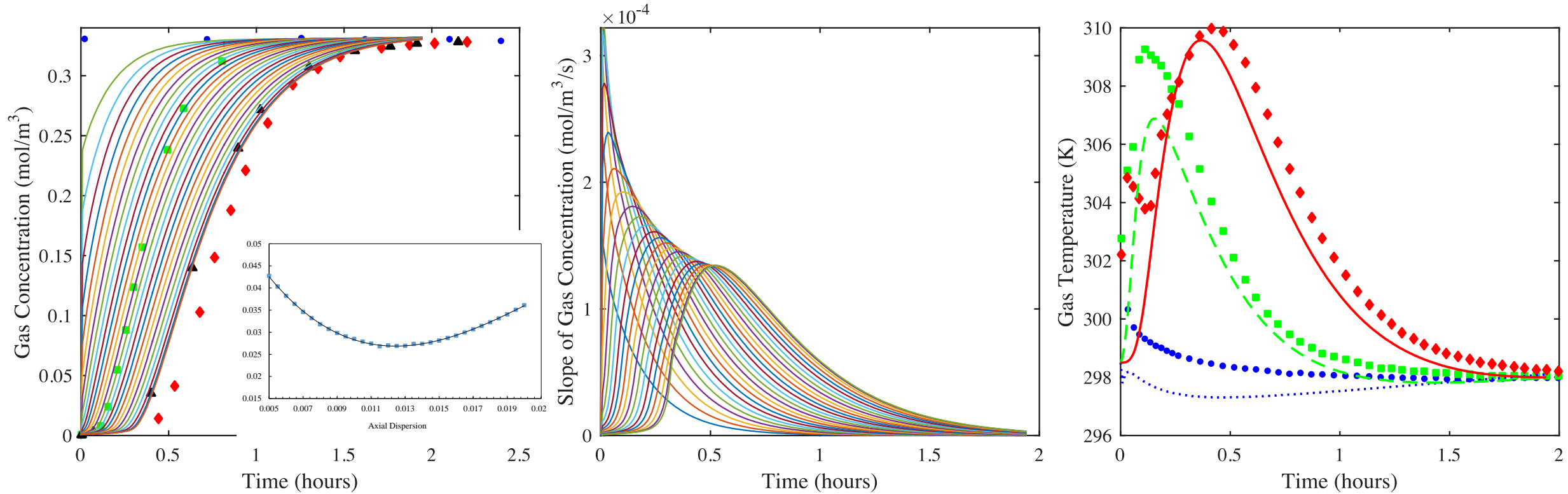


Diamonds: experimental data; dashed lines: simulations with the Edwards and Richardson correlation for axial dispersion and corresponding k_n values; dotted lines: simulations with the Wakao and Funazkri correlation for axial dispersion and corresponding k_n values.

Fits of the 1-D axial dispersed plug flow model to the 97.5% location (diamonds) experimental centerline gas-phase concentration breakthrough curves for CO₂ (left) and H₂O vapor (right) on zeolite 5A, and corresponding predictions from the model of the 2.5% (circles) and 50% (squares) locations. The saturation term in the CO₂-zeolite 5A isotherm was increased by 15%. The saturation term in the H₂O vapor-zeolite 5A isotherm was decreased by 3%. **The void fraction was reduced to 0.33 based on the Cheng distribution (Cheng *et al.*, 1991) with $C = 1.4$ and $N = 5$, as recommended by Nield and Bejan (1992)**

k_n is empirically derived via fitting to centerline concentration breakthrough curve. For this step, dispersion is taken to result from pellet effects only (no wall effects). Choice of dispersion correlation has a small impact on k_n

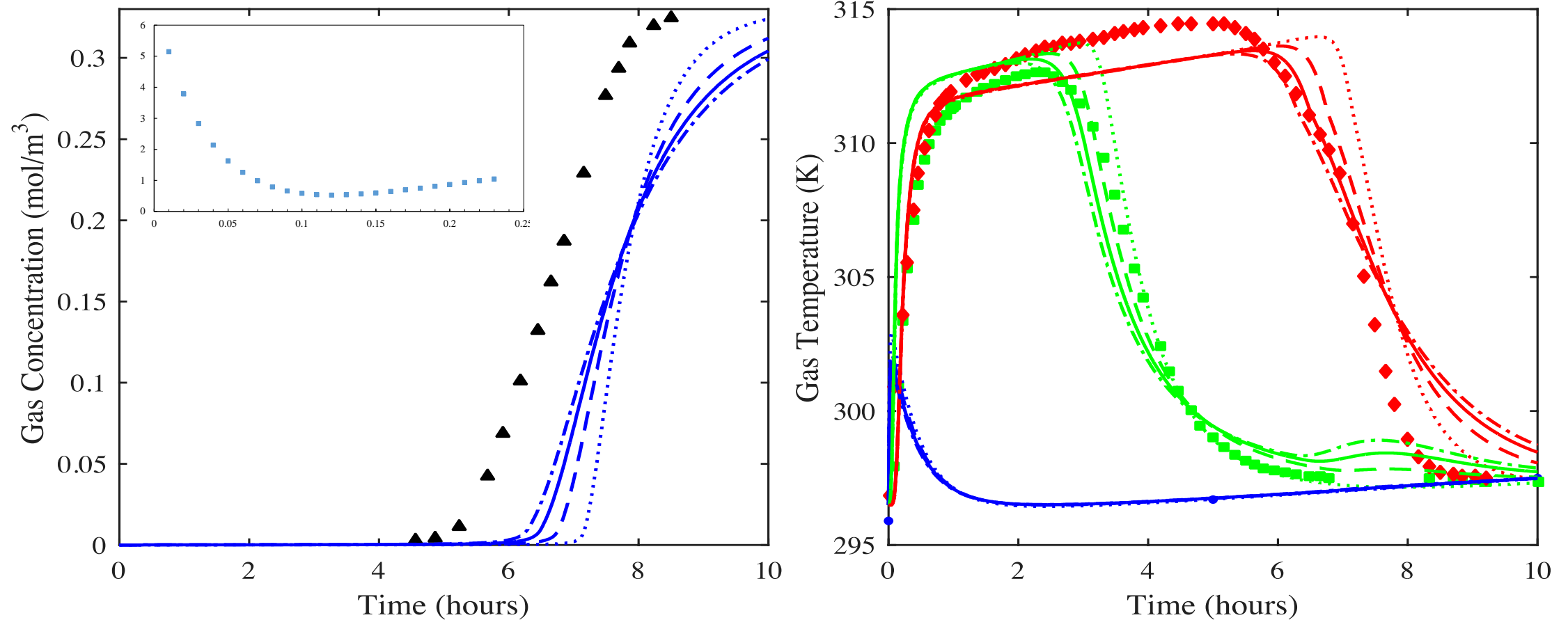
Step 3: Axial Dispersion Coefficient (CO₂ Case)



CO₂ on zeolite 5A: Fit of the 1-D axial dispersed plug flow model to the outside bed (triangles) experimental breakthrough curve using a value of D_L 7 times greater than that from the Wakao and Funazkri correlation and the fitted LDF $k_n = 0.0023 \text{ s}^{-1}$ (left panel). The reported saturation term for the CO₂-zeolite 5A isotherm was used, along with **the reported void fraction of 0.35**. Predictions from the model (lines) of the gas-phase concentration breakthrough curves at 0, 4, 8, 12, ..., 92, 96 and 100% locations in the bed are also shown in the left panel, along with the 2.5% (circles), 50% (squares) and 97.5% location (diamonds) experimental center line gas-phase concentration breakthrough curves (left panel). The corresponding derivative (or slope) of the predicted gas-phase concentration breakthrough curves in the bed are shown in the middle panel. Predictions from the model (lines) of the 2.5% (circles), 50% (squares) and 97.5% location (diamonds) experimental center line temperature profile histories are shown in the right panel.

D_L term is fit to mixed gas concentration (far downstream), but requires value 7 times the correlation value to compensate for wall channeling. Fit is specific to the size of the column; for a much larger column wall channeling may be neglected and correlated values of D_L used (but not for fixed beds with a tube to pellet ratio of 20 as in this case, or less)

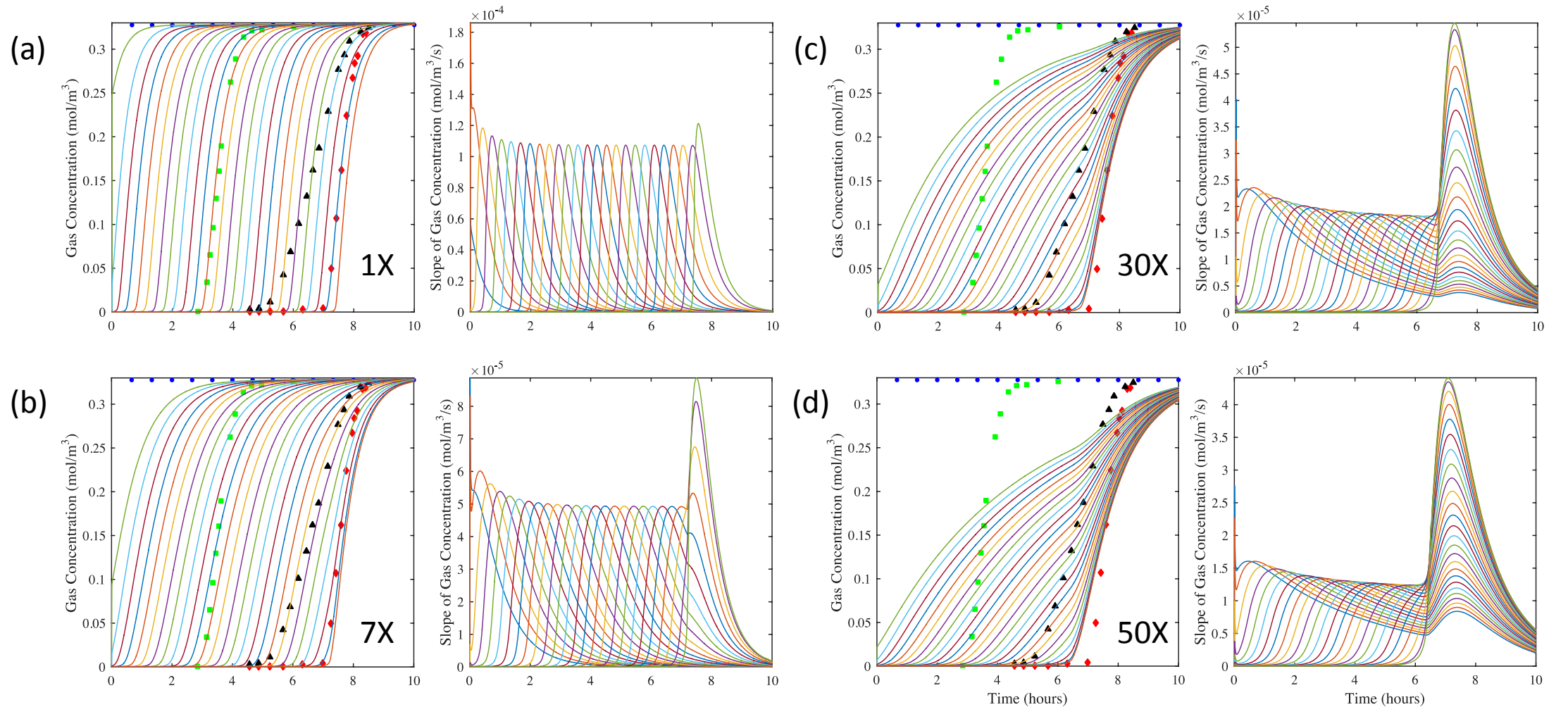
Step 3: Axial Dispersion Coefficient (H_2O Case)



H_2O vapor on zeolite 5A: Predictions from the 1-D axial dispersed plug flow model of the outside the bed (triangles) experimental breakthrough curve when varying the value of D_L . $D_L = 10$ (dotted lines), 30 (dashed lines), 50 (solid lines) and 70 (dash-dot lines) times greater than Wakao and Funazkri correlation with the LDF $k_n = 0.00083 \text{ s}^{-1}$ (left panel). The reported saturation term for the H_2O -zeolite 5A isotherm was used, along with the reported void fraction of 0.35. The corresponding predictions from the model (lines) of the 2.5% (circles), 50% (squares) and 97.5% location (diamonds) experimental center line temperature profile histories are shown in the right panel.

D_L term is fit to mixed gas concentration (far downstream), but requires value **50(!)** times the correlation value to compensate for wall channeling. However the temperature profiles deviate increasingly from the test data with increasing D_L indicating a breakdown of the axial dispersed plug flow model.

Breakthrough Sharpening and Breakdown of Constant Pattern Behavior



H₂O vapor on zeolite 5A: Predictions from the model (lines) shown in Figure 9 of the gas-phase concentration breakthrough curves at 0, 4, 8, 12, ..., 92, 96 and 100% locations in the bed (left panels). The 2.5% (circles), 50% (squares) and 97.5% location (diamonds) experimental centerline gas-phase concentration breakthrough curves are also shown for comparison in the left panels. The corresponding derivatives (or slopes) of the gas-phase concentration breakthrough curves in the bed are shown in the right panels. (a) D_L = Wakao-Funazkri correlation, and (b) $D_L = 7$, (c) 30 and (d) 50 times greater than Wakao and Funazkri correlation.

At 7X, internal concentration history slope matches mixed concentration just as for CO₂ case. This indicates that same dispersive mechanism occurs regardless of sorbate. To overcome non-physical breakthrough sharpening, D_L must be increased by 50X to decrease breakthrough slope. Expected CPB is lost entirely for this condition.

Conclusions

- Breakthrough tests with tube diameter to pellet diameter ratios of around 20 (or less), are subject to wall channeling, an mechanism not captured in standard dispersive correlations. *Breakthrough tests are generally subscale to conserve sorbent materials and gas flow equipment costs and thus frequently in this range.*
- The typical breakthrough measurement is taken far downstream, after mixing. *Fitting the mass transfer coefficient to this measurement will provide erroneous results for a larger (or smaller) diameter column due to the influence of channeling.*
- A method has been demonstrated where a centerline measurement is used to derive a mass transfer coefficient that captures physics free of wall effects and thus appropriate for scale-up to large diameter columns.
- Using the mass transfer coefficient derived above, this method uses the mixed concentration data for fitting of a dispersion coefficient D_L specific to the tube diameter, as needed for processes that utilize small diameter tubes.

Conclusions (continued)

- However fitting D_L blindly to the breakthrough curve (as apparent in many published breakthrough analyses) can, in specific cases, result in a complete breakdown of the axially dispersed plug flow model, and result in fitted coefficients that are incorrect.
- The axially dispersed plug flow equation and the Danckwerts boundary condition works well for values of dispersion within bounds of accepted correlations
- However, for specific combinations of K_d , D_L and k_n this model breaks down due to the elimination of dispersion at the outlet boundary. In these cases, significant breakthrough sharpening occurs as well as distortion of the internal concentration, deviating from the accepted CPB for these systems.